2002

Evidence for vortex pinning induced by fluctuations in the transition temperature of MgB2 superconductors

M. J. Qin
University of Wollongong, qin@uow.edu.au

Xiaolin Wang
University of Wollongong, xiaolin@uow.edu.au

Hua-Kun Liu
University of Wollongong, hua@uow.edu.au

S. X. Dou
Univeristy of Wollongong, shi@uow.edu.au

Evidence for vortex pinning induced by fluctuations in the transition temperature of MgB_2 superconductors

M. J. Qin, X. L. Wang, H. K. Liu, and S. X. Dou
Institute for Superconducting and Electronic Materials, University of Wollongong, Wollongong, New South Wales 2522, Australia
(Received 5 October 2001; published 19 March 2002)

The field-dependent critical current density $j_c(B)$ of a MgB_2 bulk sample has been obtained using magnetic measurements. The $j_c(B)$ curves at different temperatures demonstrate a crossover from single vortex pinning to small-bundle vortex pinning, when the field is larger than the crossover field B_{sb}. The temperature dependence of $B_{sb}(T)$ is in agreement with a model of randomly distributed weak pinning centers via the spatial fluctuations of the transition temperature (δT_c pinning), while pinning due to the mean-free-path fluctuations (δl pinning) is not observed.

DOI: 10.1103/PhysRevB.65.132508 PACS number(s): 74.70.Ad, 74.25.Dw, 74.25.Ha, 74.60.−w

The recent discovery of superconductivity in MgB_2 (Ref. 1) has led to intensive experimental and theoretical activities,[2–15] with the purpose of understanding the basic mechanism of superconductivity and the vortex-pinning mechanism governing the critical current density j_c in this new superconductor. Although j_c has been improved greatly since its discovery, the underlying pinning mechanism is still under investigation.

In type-II superconductors, the most important elementary interactions between vortices and pinning centers are the magnetic interaction and the core interaction.[16–22] The magnetic interaction arises from the interaction of surfaces between superconducting and nonsuperconducting material parallel to the applied field, which is usually very small in type-II superconductors with a high Ginzburg-Landau (GL) parameter κ. The core interaction arises from the coupling of the locally distorted superconducting properties with the periodic variation of the superconducting order parameter, which is usually more effective in technical type-II superconductors due to the high κ value. Two mechanisms of core pinning are predominant in type-II superconductors, i.e., δT_c and δl pinning. Whereas δT_c pinning is caused by the spatial variation of the GL coefficient α associated with disorder in the transition temperature T_c, variations in the charge-carrier mean free path l near lattice defects are the main cause of δl pinning.

It has been reported by Griessen *et al.*[16] that the δl pinning is dominant in both $YBa_2Cu_3O_7$ and $YBa_2Cu_4O_8$ thin films. A high κ value of 26 has been reported[10] for MgB_2, indicating that the magnetic interaction is negligible, and the core interaction is more important. However, it has not been experimentally determined whether the δl pinning or the δT_c pinning is the dominant mechanism in MgB_2. The purpose of this paper is to report measurements of j_c of this new material to achieve an understanding of the vortex-pinning mechanism and to demonstrate that in MgB_2 governed by bulk pinning, δT_c is the only important pinning mechanism.

All measurements have been performed using quantum design PPMS on a MgB_2 bulk sample with $T_c = 38.6$ K and dimensions of $2.18\times2.76\times1.88$ mm^3, which was prepared by conventional solid-state reaction.[23,24]

Figure 1 shows the hysteresis loops of the MgB_2 sample every 2 K in the 14–36 K range. The results at lower temperatures, which have large flux jumping,[23] are not shown here. The symmetric hysteresis loops with respect to the magnetic field indicate the dominance of bulk pinning up to temperatures near T_c, rather than surface barrier. As a comparison, we show in the inset of Fig. 1 the hysteresis loop of a pressed MgB_2 sample at 5 K. This sample is fabricated by pressing the MgB_2 powder into a pellet without sintering. The loop is highly asymmetric, showing a large reversible magnetization resulting from the surface current. The surface barrier has also been observed by Takano *et al.*[13] in their powder sample and bulk sample sintered at low temperature.

From these $M(H)$ loops, we calculate $j_c = \Delta M/a(1 - a/3b)$, with a, b the width and length of the sample perpendicular to the applied field, respectively. The resultant $j_c(B)$ curves at various temperatures are shown in a double-logarithmic plot in Fig. 2 as different symbols. As can be seen from the plateau at low field, j_c initially has a weak dependence on the field. When the field is increased beyond a crossover field, it begins to decrease quickly. The crossover field decreases with increasing temperature. Further increasing the field results in a faster drop in j_c near the irrevers-

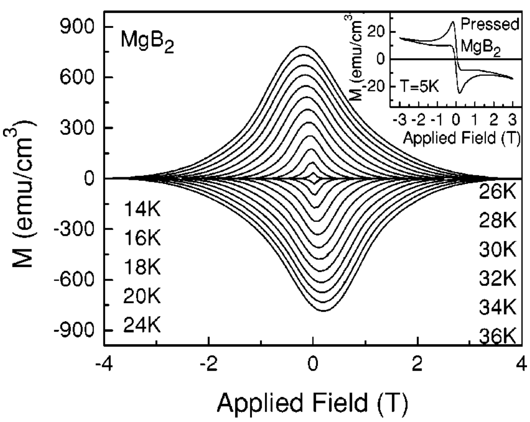

FIG. 1. Hysteresis loops of the MgB_2 sample taken every 2 K in the 14–36 K range. Results at lower temperatures are not shown because of large flux jumping. Inset shows the hysteresis loop of a pressed MgB_2 sample at 5 K, showing large reversible magnetization from the surface current.

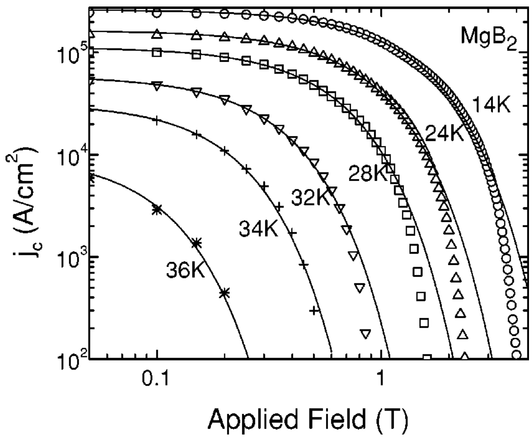

FIG. 2. j_c of the MgB_2 sample at various temperatures indicated by different symbols. Solid lines are fitting curves using Eq. (4).

ibility line, which is obtained by using a criterion of $j_c = 100\ \mathrm{A/cm}^2$ and shown as open circles in Fig. 3. The best fitting of the data yields,

$$B_{\rm irr}(t) = B_{\rm irr}(0)(1-t^2)^{3/2}, \tag{1}$$

shown as solid line in Fig. 3, with $t = T/T_c$. For high-temperature superconductors, a $(1-t)^{3/2}$ behavior is usually observed[25] and has been explained by means of giant flux creep.[26,27] The $(1-t)^{3/2}$ law is actually an approximation of the $(1-t^2)^{3/2}$ law as $t \to 1$. Also plotted in the figure is the $B_{c2}(T)$ data taken from Takano's work, showing that $B_{\rm irr}$ is well below B_{c2}. Therefore, giant flux creep also plays an important role in the new superconductor MgB_2.

$j_c(B)$ characteristics very similar to those shown in Fig. 2 have been observed by other groups.[3,14,15] Based on different physical assumptions on summation of the elementary pinning force f_p to obtain the macroscopic pinning force F_p, different pinning models yield different $j_c(B)$ characteristics. The simplest model is the direct summation of f_p to have $F_p = j_c B = n_p f_p$, where n_p is the density of pinning centers. When the influence of the flux-line lattice is taken into account, one have $F_p = j_c B = n_p f_p^2 (u_0/f_p) d/a_0^2$, where u_0 is the maximum distortion of the flux-line lattice, caused by a point finning force f_p, d is the range of the pinning force, typically of the order of ξ, and a_0 the flux-line lattice constant. These two strong pinning models yield $j_c \propto B^{-1}$ and $j_c \propto B^{-0.5}$, respectively. Due to the large densities of the pins n_p and small f_p, these two models are not representative for most real pinning systems.[28] For randomly distributed weak pinning centers, the F_p can be estimated using the basic concept of collective pinning,[29] which has been proved to be very successful in most real pinning systems,

$$F_p = j_c B = \sqrt{\frac{W}{V_c}} = \sqrt{\frac{W}{R_c^2 L_c}} \tag{2}$$

with the correlation volume $V_c = R_c^2 L_c$, the correlation lengths R_c perpendicular to the field direction and L_c along the vortex line, and the pinning parameter $W = n_p \langle f_p^2 \rangle$. R_c and L_c depend on the applied field, the dimension of the flux-line lattice [three dimensional (3D) or 2D], and the elasticity or plasticity of the flux-line lattice. For the 3D elastic flux-line lattice, it has been derived by Blatter *et al.*[17] that j_c is field independent when the applied field is lower than the crossover field $B_{\rm sb}$ (single vortex pinning)

$$B_{\rm sb} = \beta_{\rm sb} \frac{j_{\rm sv}}{j_0} B_{c2} \tag{3}$$

where $\beta_{\rm sb} \approx 5$ is a constant, $j_0 = 4B_c/3\sqrt{6}\mu_0\lambda$ the depairing current, $B_c = \Phi_0/2\sqrt{2}\pi\lambda\xi$ the thermodynamic critical field, $B_{c2} = \mu_0\Phi_0/2\pi\xi^2$ the upper critical field, and $j_{\rm sv}$ the critical current density in the single vortex-pinning regime. When $B > B_{\rm sb}$ (small-bundle pinning), $j_c(B)$ follows an exponential law,

$$j_c(B) \approx j_c(0)\exp\left[-\left(\frac{B}{B_0}\right)^{3/2}\right]. \tag{4}$$

When $B > B_{\rm lb} = \beta_{\rm lb} B_{c2}(j_{\rm sv}/j_0)[\ln(\kappa^2 j_{\rm sv}/j_0)]^{2/3}$ (where $\beta_{\rm lb}$ is a constant ≈ 2), this large bundle-pinning regime is governed by a power law $j_c(B) \propto B^{-3}$. The 2D elastic flux-line lattice shows single pancake pinning at low magnetic fields with field independent j_c, then a 2D collective-pinning region at higher fields with $j_c \propto 1/B$. For fields higher than a crossover field $B_b^{\rm 3D}$, three-dimensional pinning is predicted.

From the $j_c(B)$ curves shown in Fig. 2, it is expected that the 3D elastic pinning model may explain the dominant pinning mechanism in MgB_2. We, therefore, use Eq. (4) to fit the $j_c(B)$ curves, with fitting parameters $j_c(0)$ and B_0. The fitting results are shown as solid lines in Fig. 2. At intermediate fields, Eq. (4) fits the experimental data very well, while deviations from the fitting curves can be observed at both low and high fields. A clearer plot is shown in Fig. 4, where the $j_c(B)$ curve at 24 K is shown in a double-logarithmic plot of $-\log[j/j(B=0)]$ vs the applied field, which clearly shows a straight line at intermediate fields. The deviation at low fields is denoted as $B_{\rm sb}$, indicating the

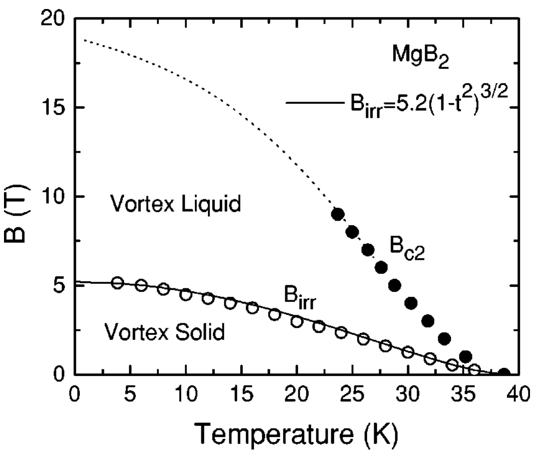

FIG. 3. B-T phase diagram of the MgB_2 sample. Open circles represent the irreversibility line obtained from Fig. 2, and the solid line is a fit to $B_{\rm irr} = 5.2(1-t^2)^{3/2}$. Solid circles represent the $B_{c2}(T)$ line from Takano's data using resistive measurements. The dashed line is just a guide to the eye.

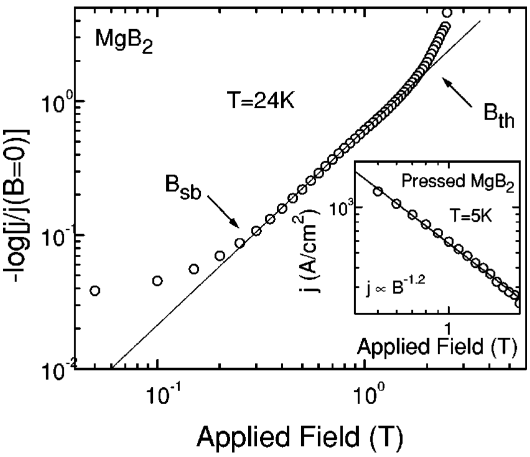

FIG. 4. j_c at 24 K in a double-logarithmic plot of $-\ln[j/j(B=0)]$ vs the applied field. The solid line is a fit using Eq. (4). $B_{\rm sb}$ indicates the crossover field from single vortex pinning to small-bundle pinning, while $B_{\rm th}$ is the crossover field to the thermal fluctuations dominated regime. Inset shows the $j_c(B)$ curve of the pressed MgB_2 sample with a large contribution from the surface current, which shows a $B^{-1.2}$ behavior.

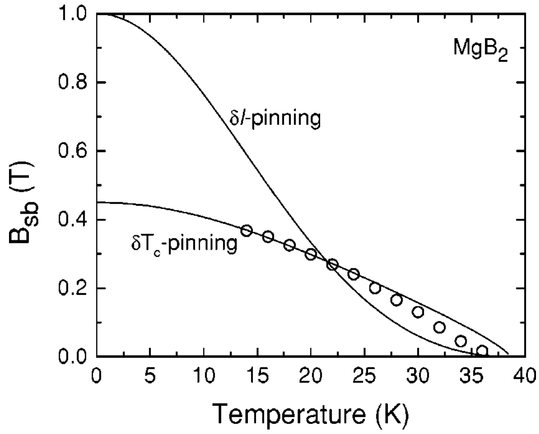

FIG. 5. Temperature dependence of the crossover field $B_{\rm sb}$. The δT_c-pinning line corresponds to Eq. (5), which is in agreement with the experimental data, while The δl-pinning line corresponds to Eq. (6), which is not in agreement with the experimental data.

crossover from the single vortex-pinning regime to the small-bundle-pinning regime. The point of deviation at high fields was first considered as the crossover field from small-bundle pinning to large-bundle pinning. However, when we fit the $j_c(B)$ data at high fields to the power law $j_c(B) \propto B^{-n}$, n is found to be as large as 20 rather than the theoretically predicted value of 3, making it unlikely that the system changes to the large-bundle-pinning regime. As the high-field deviation is very close to the irreversibility line, which results from giant flux creep, it is likely that the deviation at high field may result from large thermal fluctuations, which lead to the rapid decrease in j_c, and, therefore, is denoted as $B_{\rm th}$. The inset of Fig. 4 shows the $j_c(B)$ of the pressed sample at 5 K in a double-logarithmic plot, which indicates that when the surface pinning is important, the exponential drop in $j_c(B)$ [see Eq. (4)] no longer applies, but a power law $j_c(B) \propto B^{-1.2}$ is obvious.

The crossover field $B_{\rm sb}$ as a function of temperature is shown in Fig. 5 as open circles. We now compare the experimental data with theoretical predictions to get some insight into the pinning mechanism in MgB_2. Using $\lambda \propto (1-t^4)^{-1/2}$ and $\xi \propto [(1+t^2)/(1-t^2)]^{1/2}$, Griessen *et al.* have found that for δl pinning the critical current density in the single vortex-pinning regime $j_{\rm sv} \propto (1-t^2)^{5/2}(1+t^2)^{-1/2}$, while for δT_c pinning $j_{\rm sv} \propto (1-t^2)^{7/6}(1+t^2)^{5/6}$. Inserting all these expressions into Eq. (3), we have

$$B_{\rm sb}=B_{\rm sb}(0)\left(\frac{1-t^2}{1+t^2}\right)^{2/3} \qquad (5)$$

for δT_c pinning, and

$$B_{\rm sb}=B_{\rm sb}(0)\left(\frac{1-t^2}{1+t^2}\right)^{2} \qquad (6)$$

for δl pinning. The lines corresponding to Eqs. (5) and (6) are indicated as δT_c pinning and δl pinning, respectively, in Fig. 5. The central result of this paper is the remarkably good agreement found between $B_{\rm sb}$ and the corresponding δT_c-pinning line in the figure. In sharp contrast, the δl-pinning line shown in Fig. 5 is in total disagreement with the experimental data.

Having derived the crossover fields $B_{\rm sb}$ and $B_{\rm th}$, we reconstruct the B-T phase diagram shown in Fig. 3. The final B-T phase diagram is shown in Fig. 6. The vortex solid region is divided into three smaller regions. Single vortex pinning governs the region below $B_{\rm sb}$, between $B_{\rm sb}$ and $B_{\rm th}$, small-bundle pinning becomes dominant, while between $B_{\rm th}$ and $B_{\rm irr}$, thermal fluctuations are more important. Large-flux-bundle pinning is not observed in MgB_2, but may be concealed by the thermal fluctuation effects.

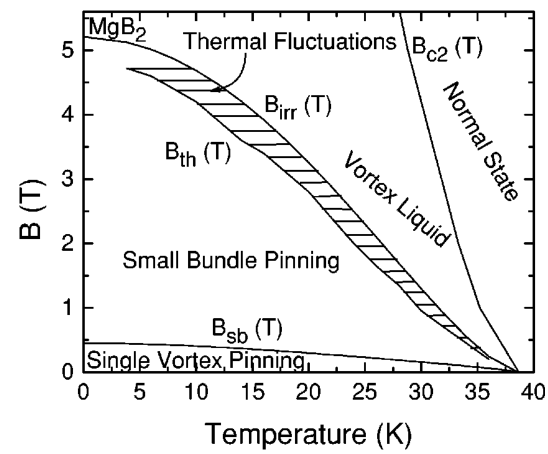

FIG. 6. B-T phase diagram of MgB_2. $B_{\rm sb}(T)$ is the fitting curve of Eq. (3) to the experimental data (see Fig. 5). $B_{\rm irr}(T)$ is the fitting curve of Eq. (1) to the experimental data (see Fig. 3). $B_{\rm th}$ is the crossover field to thermal dominant region (see Fig. 5). Again the $B_{c2}(T)$ line is taken from Takano's data using resistive measurements.

In summary, we have found strong evidence for δT_c pinning, i.e., pinning via the spatial fluctuations in the transition temperature, in MgB_2, while δl pinning, i.e., pinning via the spatial fluctuations of the charge-carrier mean free path, is not observed. The *B*-*T* phase diagram of the MgB_2 sample has been derived, showing that at low fields below B_{sb} the system is dominated by single vortex pinning and changes to smaller bundle pinning when $B > B_{sb}$. When $B > B_{th}$, this region in the vortex solid area is dominated by thermal fluctuations.

The authors would like to thank the Australian Research Council for financial support.

[1] J. Nagamatsu, N. Nakagawa, T. Maranaka, Y. Zenitani, and J. Akimitsu, Nature (London) **410**, 63 (2001).
[2] D. C. Larbalestier, M. O. Rikel, L. D. Cooley, A. A. Polyanskii, J. Y. Jiang, S. Patnaik, X. Y. Cai, D. M. Feldmann, A. Gurevich, A. A. Squitieri, M. T. Naus, C. B. Eom, E. E. Hellstrom, R. J. Cava, K. A. Regan, N. Rogado, M. A. Hayward, T. He, J. S. Slusky, P. Khalifah, K. Inumaru, and M. Haas, Nature (London) **410**, 186 (2001).
[3] Y. Bugoslavsky, G. K. Perkins, X. Qi, L. F. Cohen, and A. D. Caplin, Nature (London) **410**, 563 (2001).
[4] D. G. Hinks, H. Claus, and J. D. Jorgensen, Nature (London) **411**, 457 (2001).
[5] Y. Bugoslavsky, L. F. Cohen, G. K. Perkins, M. Polichetti, T. J. Tate, R. Gwilliam, and A. D. Caplin, Nature (London) **411**, 561 (2001).
[6] S. Jin, H. Mavoori, C. Bower, and R. B. van Dover, Nature (London) **411**, 563 (2001).
[7] C. B. Eom, M. K. Lee, J. H. Choi, L. Belenky, X. Song, L. D. Cooley, M. T. Naus, S. Patnaik, J. Jiang, M. Rikel, A. Polyanskii, A. Gurevich, X. Y. Cai, S. D. Bu, S. E. Babcock, E. E. Hellstrom, D. C. Larbalestier, N. Rogado, K. A. Regan, M. A. Hayward, T. He, J. S. Slusky, K. Inumaru, M. K. Haas, and R. J. Cava, Nature (London) **411**, 558 (2001).
[8] J. S. Slusky, N. Rogado, K. A. Regan, M. A. Hayward, P. Khalifah, T. He, K. Inumaru, S. Loureiro, M. K. Haas, H. W. Zandbergen, and R. J. Cava, Nature (London) **410**, 343 (2001).
[9] P. C. Canfield, D. K. Finnemore, S. L. Bud'ko, J. E. Ostenson, G. Lapertot, C. E. Cunningham, and C. Petrovic, Phys. Rev. Lett. **86**, 2423 (2001).
[10] D. K. Finnemore, J. E. Ostenson, S. L. Bud'ko, G. Lapertot, and P. C. Canfield, Phys. Rev. Lett. **86**, 2420 (2001).
[11] S. L. Bud'ko, C. Petrovic, G. Lapertot, C. E. Cunningham, and P. C. Canfield, M. H. Jung, A. H. Lacerda, Phys. Rev. B **63**, 220503 (2001).
[12] Herbert Schmidt, J. F. Zasadzinski, K. E. Gray, and D. G. Hinks, Phys. Rev. B **63**, 220504 (2001).
[13] Y. Takano, H. Takeya, H. Fujii, H. Kumakura, T. Hatano, K. Togano, H. Kito, H. Ihara, cond-mat/0102167 (unpublished).
[14] H. H. Wen, S. L. Li, Z. W. Zhao, Y. M. Ni, Z. A. Ren, G. C. Che, Z. X. Zhao, cond-mat/0103521 (unpublished).
[15] Amish G. Joshi, C. G. S. Pillai, P. Raj, S. K. Malik, cond-mat/0103302 (unpublished).
[16] R. Griessen, Wen Hai-hu, A. J. J. van Dalen, B. Dam, J. Rector, and H. G. Schnack, Phys. Rev. Lett. **72**, 1910 (1994).
[17] G. Blatter, M. V. Feigel'man, V. B. Geshkenbein, A. I. Larkin, V. M. Vinokur, Rev. Mod. Phys. **66**, 1125 (1994).
[18] Roger Wördenweber, Rep. Prog. Phys. **62**, 187 (1999).
[19] E. V. Thuneberg, Cryogenics **29**, 236 (1989).
[20] E. V. Thuneberg, J. Kurkijarvi, D. Rainer, Phys. Rev. Lett. **48**, 1853 (1982).
[21] C. J. van der Beek and P. H. Kes, Phys. Rev. B **43**, 13 032 (1991).
[22] P. H. Kes, Physica C **185-189**, 288 (1991).
[23] S. X. Dou, X. L. Wang, J. Horvat, D. Milliken, E. W. Collings, and M. D. Sumption, cond-mat/0102320 (unpublished).
[24] M. J. Qin, X. L. Wang, S. Soltanian, A. H. Li, H. K. Liu, and S. X. Dou, Phys. Rev. B **64**, 060505(R) (2001).
[25] K. A. Müller, M. Takashige, and J. G. Bednorz, Phys. Rev. Lett. **58**, 1143 (1987).
[26] Y. Yeshurun and A. P. Malozemoff, Phys. Rev. Lett. **60**, 2202 (1988).
[27] M. Tinkham, Phys. Rev. Lett. **61**, 1658 (1988).
[28] E. H. Brandt, Rep. Prog. Phys. **58**, 1465 (1995).
[29] A. I. Larkin and Yu. N. Ovchinnikov, J. Low Temp. Phys. **34**, 409 (1979).